

Modeling dark signal of CMOS image sensors irradiated by reactor neutron using Monte Carlo method

Yuanyuan XUE, Zujun WANG*, Wei CHEN*, Baoping HE, Zhibin YAO, Minbo LIU, Jiangkun SHENG, Wuying MA, Guantao DONG & Junshan JIN

*State Key Laboratory of Intense Pulsed Irradiation Simulation and Effect,
Northwest Institute of Nuclear Technology, Xi'an 710024, China*

Received 28 July 2017/Revised 21 September 2017/Accepted 20 October 2017/Published online 27 April 2018

Abstract The dark signal degradation of the CMOS image sensor (CIS) was induced by neutron radiation, and it was modeled by Geant4, which is a three-dimensional Monte Carlo code. The simplified model of the CIS array was established according to the actual pixel geometry, material, and doping concentration. Nuclear elastic interaction and capture interaction were included in the physical processes, and the displacement damage dose in the space charge region of the pixel was calculated. The mean dark signal and dark signal distribution were modeled using Geant4, and the physical mechanisms were analyzed. The modeling results were in good agreement with the experimental and theoretical results.

Keywords modeling, CIS, neutron radiation, dark signal, Geant4

Citation Xue Y Y, Wang Z J, Chen W, et al. Modeling dark signal of CMOS image sensors irradiated by reactor neutron using Monte Carlo method. *Sci China Inf Sci*, 2018, 61(6): 062405, <https://doi.org/10.1007/s11432-017-9323-0>

1 Introduction

In comparison with charge coupled devices (CCDs), CMOS image sensors (CISs) [1–5] have a lot of advantages, such as better electro-optical performance, lower power consumption, and higher tolerance to the radiation environment. Due to such good performances, CISs are now widely used in star tracking, medical imaging, space remote sensing, and other scientific fields. When CISs are operated in such harsh radiation environments, they incur damages by particles or rays, such as protons, neutrons, electrons, γ rays; this led to image quality degradation or even functional failure.

Dark signal is one of the most important parameters of CISs, and many studies have already been dedicated to analyzing the effects of radiation on CIS signals. Goiffon et al. [6, 7] studied the dark signal increase induced by total ionization dose (TID) damage in 3 transistor (T) conventional pixels and 4 T pinned photodiode (PPD) pixels of CISs. Virmondois et al. [8, 9] reported the displacement damage effects on the dark current of CISs induced by proton and neutron irradiation, and empirical models were established in order to evaluate the dark current distribution. Wang et al. [10, 11] reported the TID effects on CISs. The mean dark signal, dark signal non-uniformity (DSNU), dynamic range and output signal voltage versus the TID were presented, and the degradation mechanisms were also analyzed. However,

* Corresponding author (email: wangzujun@nint.ac.cn, chenwei@nint.ac.cn)

fewer studies have focused on the neutron radiation effects on the dark signal of CISs, especially using Monte Carlo method.

In this paper, the neutron radiation effects on the dark signals of the PPD CIS were investigated. The radiation tests were carried out at Xi'an pulse reactor facility. The CIS was exposed to 1 MeV of neutron-equivalent fluence of 1×10^{11} and 2×10^{11} n/cm². The geometry model of the CIS was established, and the displacement damage dose (D_d) in the space charge region caused by neutron was calculated by Geant4¹⁾ [12], a three-dimensional Monte Carlo code. The degradation of the mean dark signal, DSNU, and dark signal distribution versus neutron fluence were analyzed. This study provides a new approach towards predicting the degradation of the CIS induced by the neutron displacement damage under complicated radiation environments, and it offers good understanding on neutron induced degradation mechanisms.

2 Experimental details

The CIS under investigation is manufactured in the standard 0.18- μ m CMOS technology with PPD pixels. The shallow trench isolation (STI) thickness is approximately 1 μ m. The image array consists of 2048 \times 2048 pixels, and the pixel size is 11 μ m \times 11 μ m. The photodiode area is approximately 49 μ m², and the space charge region is approximately 78.4 μ m³. The low dark signal, low noise, and high dynamic range make the CIS suitable for being used in many scientific applications.

The CIS was irradiated by neutron at the Xi'an pulse reactor facility. The neutron flux was approximately 1.33×10^8 n/(cm²·s). The ratio of n/ γ was measured and provided by the staff of the radiation facility. The TID was measured by dosimeter, and the neutron fluence was measured by activation foil. The value of the n/ γ was approximately 4.19×10^9 n/(cm²·rad (Si)), which ensures that the TID effects could be neglected under this radiation environment (only displacement damage effects were considered). The CIS was exposed to 1 MeV of neutron-equivalent fluence of 1×10^{11} and 2×10^{11} n/cm². The CIS was unbiased during the irradiation and was measured pre- and post- radiation according to the 1288 standard of the European Machine Vision Association (EMVA) [13].

3 Monte Carlo modeling details

When the neutron passes through the material, it can dislodge atoms from their normal lattice location and create vacancies and interstitials. The combination of a vacancy and an adjacent interstitial is known as a Frenkel pair, while two adjacent vacancies from a defect are referred to as the divacancy [14]. All of these are called defects and could induce the degradation of electronic and optical CIS properties, such as the mean dark signal, DSNU, and dark signal distribution.

The 3D Monte Carlo code Geant4 was used to model the dark signal degradation of the CIS after neutron radiation (as shown in Figure 1). Geant4 is a platform for the simulation of the passage of particles through matter, by utilizing Monte Carlo methods. It is the successor of the GEANT series of software toolkits developed by European Organization for Nuclear Research (CERN), and it is the first to use an object oriented programming language (C++). It has been used in a large number of experiments and projects in a variety of application domains, including high energy physics, astrophysics, space science, medical physics, and radiation protection [9,10]. The geometry model was established according to pixel geometry, material, and doping concentration. The sensitive volume of the CIS is the space charge region, and the width of space charge region (W) is given as

$$W = \left\{ \frac{2\varepsilon(V_{bi} + V_R)}{e} \left[\frac{N_a + N_d}{N_a N_d} \right] \right\}^{1/2}, \quad (1)$$

where ε is the dielectric constant, V_{bi} is the built-in potential barrier, V_R is the magnitude of applied reverse-biased voltage, e is the electron charge, N_a is the acceptor concentration, and N_d is the donor

1) Geant4. <http://geant4.web.cern.ch/geant4>.

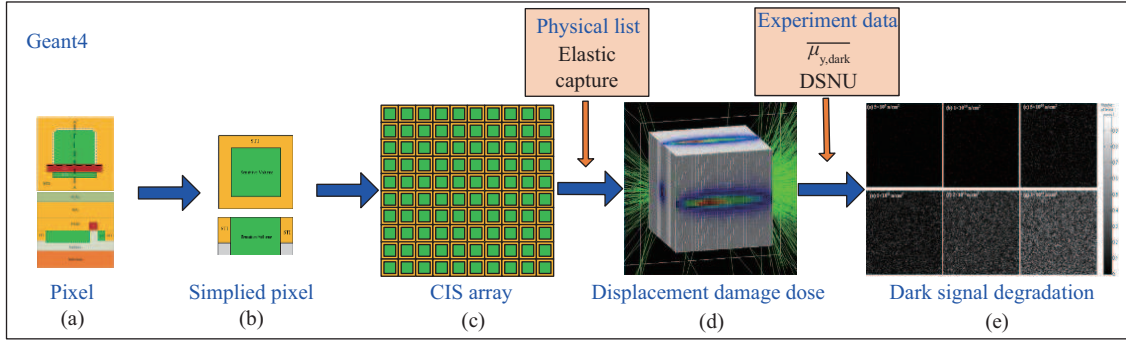


Figure 1 (Color online) Schematic of global modeling project.

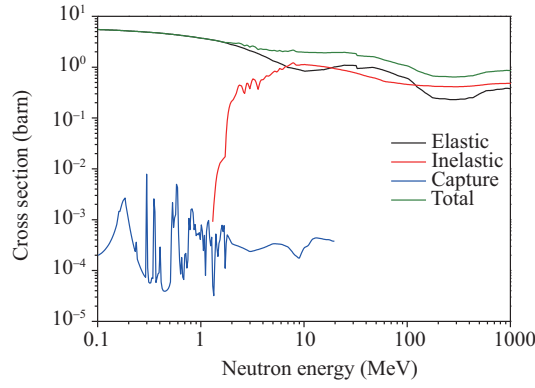


Figure 2 (Color online) Cross section of neutron for Si.

concentration. V_R is given as

$$V_R = V_t \ln \left(\frac{N_a N_d}{n_i^2} \right), \quad (2)$$

where $V_t = kT/e$ is the thermal voltage, and n_i is the intrinsic carrier concentration. The cross section of the space charge region could be calculated according to the fill factor of the CIS. Therefore, the sensitive volume was approximately $7 \mu\text{m} \times 7 \mu\text{m} \times 1.6 \mu\text{m}$. The gate oxide did not exceed 7 nm, and the STI thickness was approximately 1 μm . The pixel size was $11 \mu\text{m} \times 11 \mu\text{m}$. The sensitive volume was centrally arranged in the pixel, as shown in Figure 1(b) (passivation layers, aluminum layer, substrate, were neglected). In order to model the DSNU and dark signal distribution, the CIS array was defined and replicated as the actual layout with 100×100 pixels. In order to show it more vividly, the diagram of the 10×10 pixels architecture for modeling was shown in Figure 1(c). The cross section of the neutron for Si (92.23% of ^{28}Si , 4.68% of ^{29}Si , and 3.09% of ^{30}Si) was calculated with Geant4, as shown in Figure 2. The cross section of the 1 MeV neutron for Si was approximately 4.5475 barns. The elastic cross section was 4.5472 barns; inelastic cross section was 0 barns; capture cross section was 0.3285 mbarns, and fission cross section was 0 barns. Therefore, the nuclear elastic and capture interactions were added to the physical list of Geant4. The D_d in the space charge region of the CIS with neutron fluences of 5×10^9 , 1×10^{10} , 5×10^{10} , 1×10^{11} , 2×10^{11} , and 3×10^{11} n/cm² were calculated.

4 Results and discussion

4.1 Mean dark signal increase

The mean dark signal stands for the output signal of the CIS when it is not exposed to light. It is one of the most important parameters that can be used to estimate the displacement damage effects induced

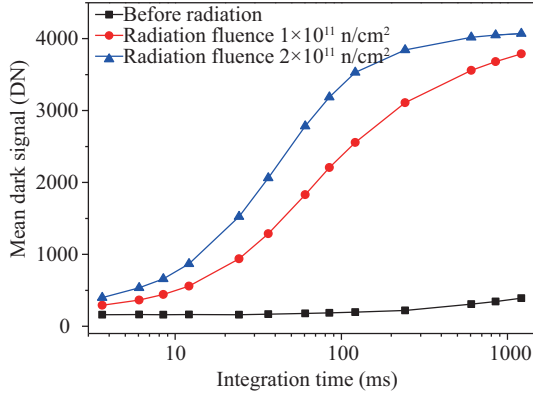


Figure 3 (Color online) Mean dark signal of CIS versus integration time pre- and post- radiation.

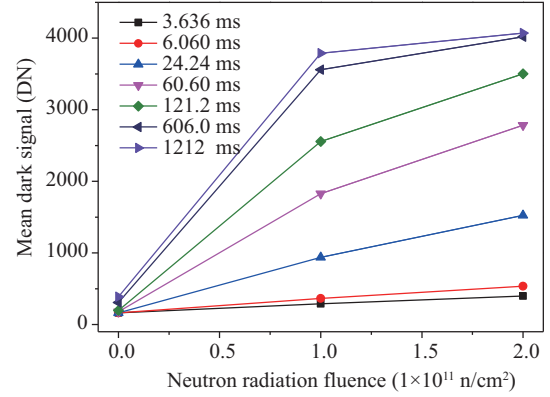


Figure 4 (Color online) Mean dark signal versus neutron radiation fluence at different integration times.

by neutrons on the CIS. The dark signal is given as follows [13]:

$$\mu_{y,\text{dark}} = \mu_{y_0,\text{dark}} + \mu_{I,\text{dark}} t_{\text{exp}}, \quad (3)$$

where $\mu_{y,\text{dark}}$ is the dark signal at a given integration time (t_{exp}), $\mu_{y_0,\text{dark}}$ is the dark signal for integration time zero, $\mu_{I,\text{dark}}$ is the sensor dark current, and t_{exp} is the integration time. Therefore, the dark signal increases with the increase of integration time. The mean dark signal is given as follows [13]:

$$\overline{\mu_{y,\text{dark}}} = \frac{1}{MN} \sum_{m=0}^{M-1} \sum_{n=0}^{N-1} \mu_{y,\text{dark}}[m][n], \quad (4)$$

where M and N are the number of rows and columns of the image, and m and n are the row and column indices of the array, respectively. The mean dark signal was measured pre- and post- radiation.

Figure 3 shows the mean dark signal of CIS versus the integration time pre- and post- radiation. The mean dark signal increases as the integration time increases at the same radiation fluence. Before neutron radiation, there are some bulk defects in the space charge region, or somewhere near the space charge region, which are introduced in the production enhancing thermal generation; these defects would produce the dark signal. Since the number of defects is less, the mean dark signal increases slowly and appears to be linearly related to integration time. After neutron radiation, there are plenty of bulk defects produced in the space charge region, which leading to the remarkable increase of the mean dark signal as the integration time increases. Furthermore, the mean dark signal appears to be proportional to integration time when it is small, and the mean dark signal growth of CIS decreases with the increase of integration time when it is big. When the CIS is radiated by the neutron, some pixels are damaged and the dark signal increases dramatically with integration time. However, some of the pixels are not damaged by neutron. When the integration time is big enough, the mean dark signal of the damaged pixels reach saturation and not increase with increasing integration time. This would lead to the decrease of mean dark signal growth.

Figure 4 shows the mean dark signal versus neutron radiation fluence at different integration times. When the integration time not exceed 24.24 ms, the mean dark signal appears to be proportional to the neutron radiation fluence. However, when the integration time is bigger, the mean dark signal is not linear with neutron radiation fluence.

In comparison with displacement damage effects, the TID effects have a little influence on the behavior of CIS, and they are considered as negligible in this study. The displacement damage effects on the CIS dark signal are connected to the D_d in the sensitive volume of the pixel. The D_d is related to the Non ionizing energy loss (NIEL) and neutron fluence $\Phi(E)$ and given as follows [14]:

$$D_d = \text{NIEL}(E) \times \Phi(E). \quad (5)$$

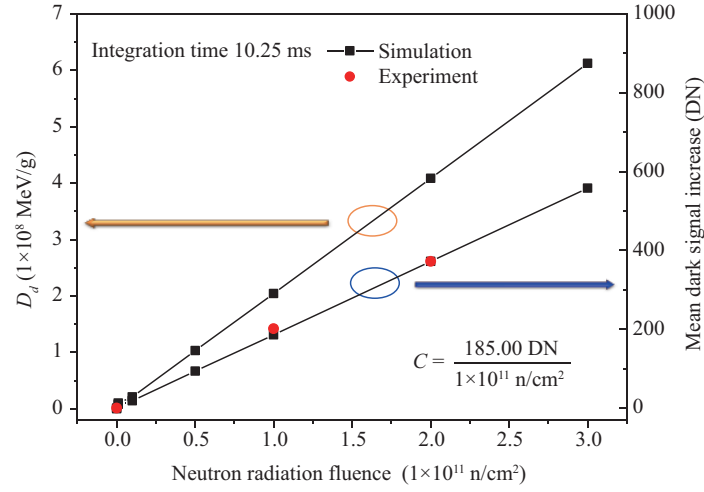


Figure 5 (Color online) Displacement damage dose (D_d) and mean dark signal increase versus neutron radiation fluence.

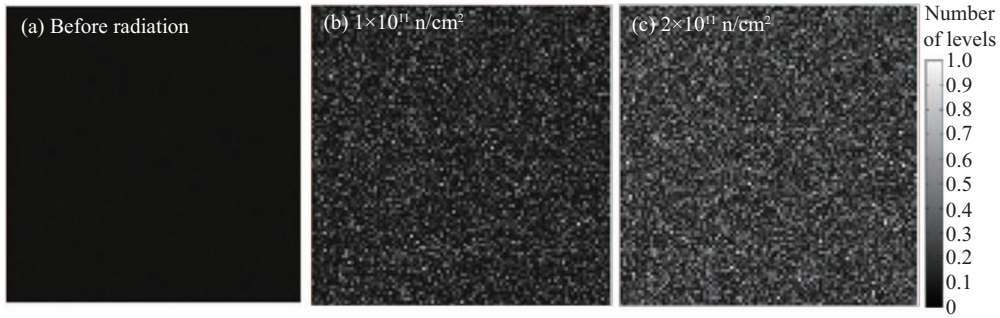


Figure 6 Captured raw images of CIS before and after neutron radiation when the integration time is approximately 10.25 ms. (a) Before radiation; (b) neutron radiation fluence: 1×10^{11} n/cm 2 ; (c) neutron radiation fluence: 2×10^{11} n/cm 2 .

The mean dark signal increase is induced by neutrons and can be expressed as follows [15]:

$$\Delta \overline{\mu_{y,\text{dark}}} = C \times D_d, \tag{6}$$

where C is a damage factor constant when integration time, radiation source, and environmental temperature are not charged. Therefore, the mean dark signal increase is in line with D_d . This also agrees with the Srour’s universal damage factor model to estimate the dark signal increase in relevance to displacement damage [16].

Figure 5 describes the D_d and the mean dark signal increase versus neutron radiation fluence when the integration time is approximately 10.25 ms. The D_d and mean dark signal increase appears to be approximately proportional to the radiation fluence, and the modeling results are in good agreement with the experimental results. The C value is approximately 185.00 DN/(1×10^{11} n/cm 2). Therefore, we can use this method for predicting the mean dark signal increase of the CIS caused by neutron displacement damage.

Figure 6 presents the captured raw images of the CIS pre- and post- neutron radiation when the integration time is approximately 10.25 ms: (a) before radiation, (b) neutron radiation fluence: 1×10^{11} n/cm 2 , and (c) neutron radiation fluence: 2×10^{11} n/cm 2 . Figure 7 presents the modeled raw images of CIS after neutron radiation when the integration time is approximately 10.25 ms: (a) fluence: 5×10^9 n/cm 2 , (b) fluence: 1×10^{10} n/cm 2 , (c) fluence: 5×10^{10} n/cm 2 , (d) fluence: 1×10^{11} n/cm 2 , (e) fluence: 2×10^{11} n/cm 2 , and (f) fluence: 3×10^{11} n/cm 2 . From Figures 6 and 7, we can see that the modeled raw images are in good agreement with the actual captured images. After neutron radiation, there are a lot of “hot pixels” appearing in the raw CIS image, and the “hot pixel” counts increase with increasing neutron radiation fluence.

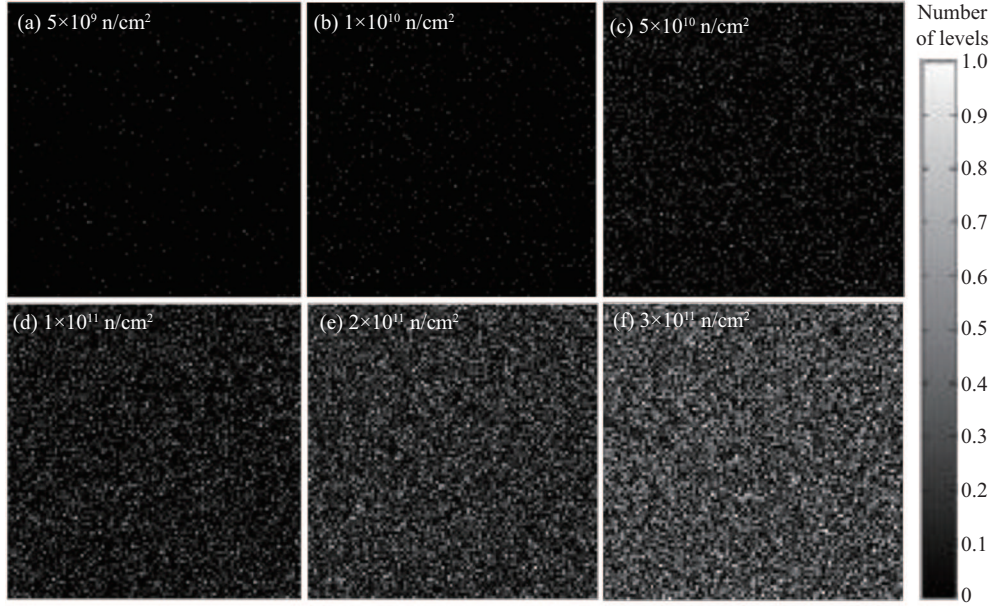


Figure 7 Modeled raw images of CIS after neutron radiation when the integration time is approximately 10.25 ms. Fluence: (a) 5×10^9 n/cm²; (b) 1×10^{10} n/cm²; (c) 5×10^{10} n/cm²; (d) 1×10^{11} n/cm²; (e) 2×10^{11} n/cm²; (f) 3×10^{11} n/cm².

4.2 DSNU increase

DSNU stands for the non-uniformity of dark signal. It originates from a somewhat different output signal from one pixel to another. The DSNU is given as follows [13]:

$$\text{DSNU} = \frac{1}{MN - 1} \sum_{m=0}^{M-1} \sum_{n=0}^{N-1} (\mu_{y,\text{dark}}[m][n] - \overline{\mu_{y,\text{dark}}})^2. \quad (7)$$

Neutron radiation not only affects the mean dark signal but also affects the DSNU. The numbers of pixels that are damaged by incident neutrons exert great DSNU influence on CIS. The mean numbers of nuclear interactions per pixel is given as follows:

$$\mu = \sigma N_a V_{\text{dep}} \Phi(E), \quad (8)$$

where σ is the cross section of the incident neutron, N_a is the material atomic density, V_{dep} is the depleted volume of the pixel. The cross section of the 1 MeV neutron that created a bulk defect in Si is approximately 4.5475 barns. Therefore, the mean number of nuclear interactions per pixel should be approximately 0.089, 0.178, 0.89, 1.78, 3.56, and 5.34 when the neutron radiation fluence is 5×10^9 – 3×10^{11} n/cm². The number of nuclear interactions per pixel can be expressed as a Poisson distribution

$$P(X = k) = \frac{\lambda^k}{k!} e^{-\lambda}, \quad k = 0, 1, 2, \dots, \quad (9)$$

where k is the number of nuclear interactions per pixel, and λ is the mean number of nuclear interactions per pixel. Therefore, the probability of nuclear interactions in CIS can be calculated by

$$P(X \neq 0) = 1 - P(X = 0). \quad (10)$$

Combined with (8), (9), and (10), we can obtain the theoretical results of the normalized number of nuclear interactions.

Figure 8 presents the normalized number of nuclear interactions in 100×100 pixels of CIS versus neutron radiation fluence. The normalized number of nuclear interactions increases vividly as neutron fluence increases. When the neutron radiation fluence is 5×10^9 n/cm², the damaged pixels do not exceed 10%.

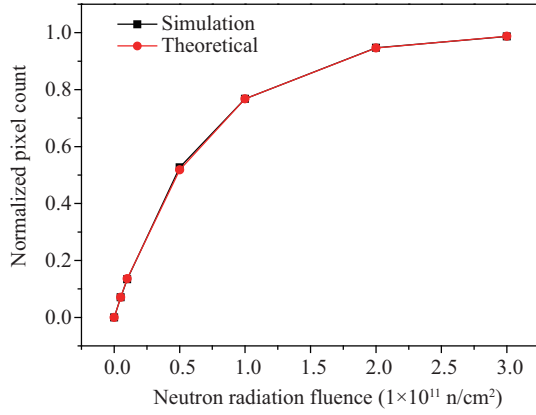


Figure 8 (Color online) Normalized number of nuclear interactions in 100×100 pixels CIS versus neutron radiation fluence.

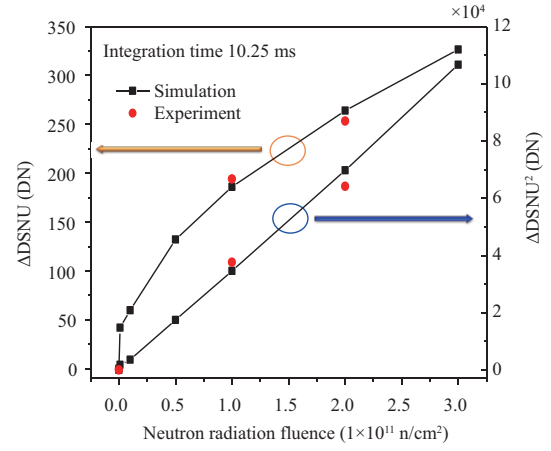


Figure 9 (Color online) DSNU and square of DSNU increase versus neutron radiation fluence.

However, when the neutron fluence is 2×10^{11} n/cm 2 , nearly all of the pixels are damaged by neutrons, which can induce a lot of “hot pixels,” as presented in Figures 6(c) and 7(f). Modeling, theoretical, and experimental results are in good agreement, which implies that there is little crosstalk effect in this CIS array when radiated with 1 MeV neutron under this integration time.

Figure 9 describes the DSNU increase and the square of the DSNU increase versus neutron radiation fluence by modeling and experiment when the integration time is approximately 10.25 ms. The DSNU increase degrades dramatically with increasing integration time, and the square of the DSNU is linear with neutron radiation fluence. The modeling results are in good agreement with experimental results. When the nuclear interaction is one per pixel in average, the probability density function of the dark current is given as follows [5]:

$$f(x) = \frac{1}{\Delta \overline{\mu_{I,\text{dark}}}} \exp\left(-\frac{x}{\Delta \overline{\mu_{I,\text{dark}}}}\right), \quad (11)$$

where x is the dark current variable, and $\Delta \overline{\mu_{I,\text{dark}}}$ is the mean dark current increase per nuclear interaction. Therefore, the probability density function of the dark signal can be expressed as follows:

$$f(y) = \frac{1}{\Delta \overline{\mu_{y,\text{dark}}}} \exp\left(-\frac{y}{\Delta \overline{\mu_{y,\text{dark}}}}\right), \quad (12)$$

where y is the dark signal variable, and $\Delta \overline{\mu_{y,\text{dark}}}$ is the mean dark signal increase per nuclear interaction. The variance of the dark signal is the same $\Delta \overline{\mu_{y,\text{dark}}}$. When the mean number of the nuclear interactions per pixel is more than one, the probability density function of the dark signal $f(Y, z)$ can be expressed as follows:

$$f(Y, z) = f(y) * f(y) \cdots f(y) * f(y), \quad (13)$$

where $*$ is the convolution symbol, and z is the mean number of nuclear interactions per pixel. The expectation of the dark signal increase is $z \times \Delta \overline{\mu_{y,\text{dark}}}$, and the variance of the dark signal increase is $z \times (\Delta \overline{\mu_{y,\text{dark}}})^2$. Therefore, the ΔDSNU^2 can be expressed as follows:

$$\Delta \text{DSNU}^2 = K \times \Phi(E), \quad (14)$$

where K is a constant. Therefore, ΔDSNU^2 is linear with neutron radiation fluence, which is in good agreement with experimental and modeling results.

Figure 10 provides the 3-D surface plot of experimental raw images: (a) before radiation, (b) neutron radiation fluence: 1×10^{11} n/cm 2 , (c) neutron radiation fluence: 2×10^{11} n/cm 2 . From Figure 10, we can

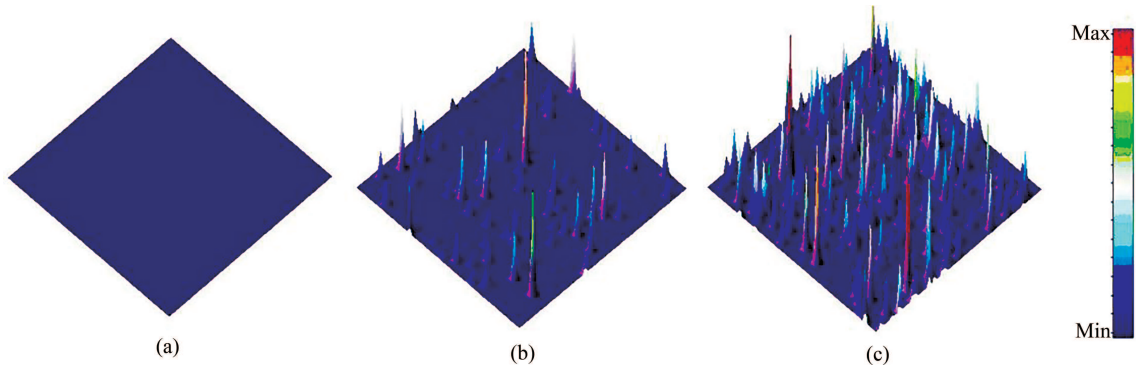


Figure 10 (Color online) The 3D surface plot of experimental raw images. (a) Before radiation; (b) neutron radiation fluence: 1×10^{11} n/cm²; (c) neutron radiation fluence: 2×10^{11} n/cm².

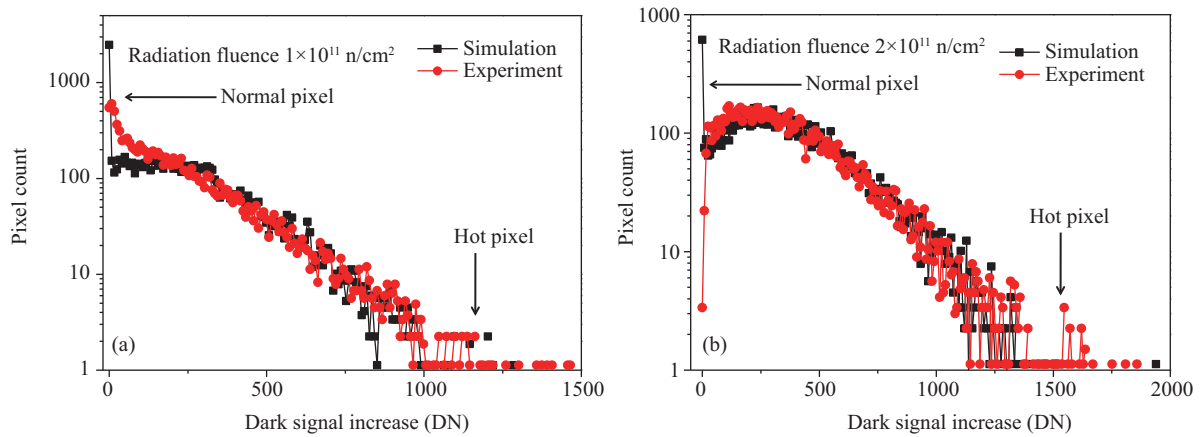


Figure 11 (Color online) Dark signal increase distributions in the CIS after neutron irradiations. (a) Fluence: 1×10^{11} n/cm²; (b) fluence: 2×10^{11} n/cm².

see that there are a lot of dark signal spikes that are induced by bulk defects produced in the space charge region after neutron radiation. The dark signal spikes would have great effects on the DSNU of the CIS. Therefore, the DSNU obviously increases after neutron radiation.

4.3 Dark signal distribution

The mean dark signal results, DSNU results and dark signal distributions, complement one another. Figure 11 displays the dark signal increase distributions in the 100×100 pixels after neutron radiation: (a) neutron radiation fluence: 1×10^{11} n/cm², and (b) neutron radiation fluence: 2×10^{11} n/cm². The black line with the square points indicates the modeling results based on Geant4; the red line with round points indicates the experimental results. The experimental data are in good agreement with the modeling data, except from the dark signal, which is close to zero. Additionally, the dark signal distributions of the experimental results, radiated by a neutron fluence of 2×10^{11} n/cm², are more appropriate to the modeling results. One possible explanation for this phenomenon is that the TID effect on the distributions of dark signal increase cannot be neglected when dark signal increase are close to zero. Based on the results from Geant4, Figure 12 shows the modeled dark signal increase distributions of CIS after neutron radiation at several radiation fluences. This can help us estimate the degradation of CIS dark signal distribution, which is exposed to 1 MeV neutron-equivalent, at different fluences.

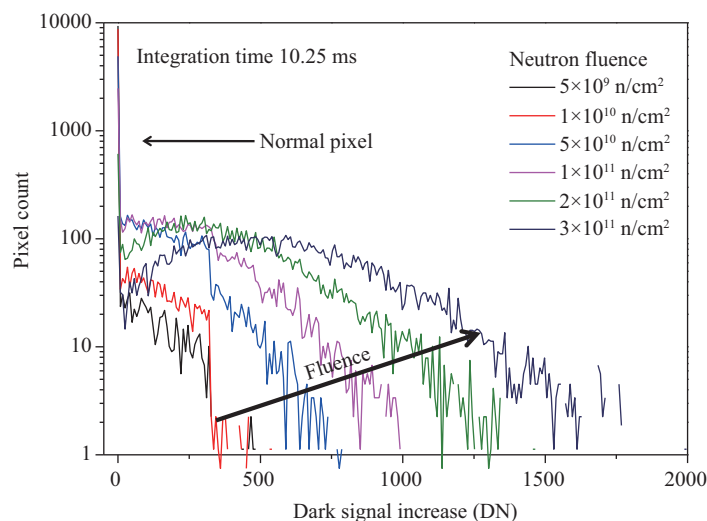


Figure 12 (Color online) Modeled dark signal increase distributions of CIS after neutron radiation at several radiation fluences.

5 Conclusion

In this study, the inducing of neutron radiation and the dark signal distribution degradation of CIS were modeled. The experiments consisted of irradiation by neutrons with different fluence, and the experimental results were analyzed. The trends of dark signal degradation were related to integration time. In order to account for the fact that most of the pixels in the CIS array do not reach saturation, in this study, we modeled the dark signal degradation when the integration time was approximately 10.25 ms. The modeled raw images, number of nuclear interactions, mean dark signal, DSNU, and dark signal distribution were in good agreement with experimental and theoretical results.

In order to extend the model and make the results more accurate, the TID effects should be taken into account. Moreover, the dark signal degradation at different integration times, in which the dark signal increase is not proportional to the radiation fluence, should be modeled later, and more experiments should be carried out in order to verify the modeling results.

Acknowledgements This work was supported by Strategic Priority Research Program of Chinese Academy of Science (Grant No. XDA15015000), National Natural Science Foundational of China (Grant No. 11690043), and Foundation of State Key Laboratory of China (Grant No. SKLIPR1610).

References

- 1 Zhou Y F, Cao Z X, Qin Q, et al. A high speed 1000 fps CMOS image sensor with low noise global shutter pixels. *Sci China Inf Sci*, 2014, 57: 042405
- 2 Zhou Y F, Cao Z X, Han Y, et al. A low power global shutter pixel with extended FD voltage swing range for large format high speed CMOS image sensor. *Sci China Inf Sci*, 2015, 58: 042406
- 3 Chen Z, Di S, Cao Z X, et al. A 256×256 time-of-flight image sensor based on center-tap demodulation pixel structure. *Sci China Inf Sci*, 2016, 59: 042409
- 4 Xue Y Y, Wang Z J, Liu M B, et al. Research on proton radiation effects on CMOS image sensors with experimental and particle transport simulation methods. *Sci China Inf Sci*, 2017, 60: 120402
- 5 Chen W, Yang H L, Guo X Q, et al. The research status and challenge of space radiation physics and application (in Chinese). *Chin Sci Bull*, 2017, 62: 978–989
- 6 Goiffon V, Virmondois C, Magnan P, et al. Identification of radiation induced dark current sources in pinned photodiode CMOS image sensors. *IEEE Trans Nucl Sci*, 2012, 59: 918–926
- 7 Goiffon V, Estribeau M, Magnan P. Overview of ionizing radiation effects in image sensors fabricated in a deep-submicrometer CMOS imaging technology. *IEEE Trans Electron Dev*, 2009, 56: 2594–2601
- 8 Virmondois C, Goiffon V, Magnan P, et al. Similarities between proton and neutron induced dark current distribution in CMOS image sensors. *IEEE Trans Nucl Sci*, 2012, 59: 927–936

- 9 Virmondois C, Goiffon V, Magnan P, et al. Displacement damage effects due to neutron and proton irradiations on CMOS image sensors manufactured in deep submicron technology. *IEEE Trans Nucl Sci*, 2010, 57: 3101–3108
- 10 Wang Z J, Liu C J, Ma Y, et al. Degradation of CMOS APS image sensors induced by total ionizing dose radiation at different dose rates and biased conditions. *IEEE Trans Nucl Sci*, 2015, 62: 527–533
- 11 Wang Z J, Ma W Y, Liu J, et al. Degradation and annealing studies on gamma rays irradiated COTS PPD CISs at different dose rates. *Nucl Instrum Meth Phys Res A*, 2016, 820: 89–94
- 12 Allison J, Amako K, Apostolakis J, et al. Geant4 developments and applications. *IEEE Trans Nucl Sci*, 2006, 53: 270–278
- 13 European Machine Vision Association (EMVA). EMVA Stand 1288. 2012
- 14 Srour J R, Palko J W. Displacement damage effects in irradiated semiconductor devices. *IEEE Trans Nucl Sci*, 2013, 60: 1740–1766
- 15 Wang Z J, Huang S Y, Liu M B, et al. Displacement damage effects on CMOS APS image sensors induced by neutron irradiation from a nuclear reactor. *AIP Adv*, 2014, 4: 077108
- 16 Srour J R, Lo D H. Universal damage factor for radiation-induced dark current in silicon devices. *IEEE Trans Nucl Sci*, 2000, 47: 2451–2459